

## Structural properties of the ferroelectric phases of a chiral liquid crystal revealed by dynamic light scattering

D. Konovalov,<sup>1</sup> H. T. Nguyen,<sup>2</sup> M. Čopič,<sup>3</sup> and S. Sprunt<sup>1</sup>

<sup>1</sup>*Department of Physics, Kent State University, Kent, Ohio 44242*

<sup>2</sup>*Centre de Recherche Paul Pascal, CNRS, Université Bordeaux I, Avenue A. Schweitzer, F-33600 Pessac, France*

<sup>3</sup>*Department of Physics, University of Ljubljana, 1000 Ljubljana, Slovenia*

(Received 4 April 2001; published 28 June 2001)

Dynamic light scattering is used to study the antiferro- and ferroelectric phases in a bulk sample of the chiral liquid crystal R-100TBBBIM7. Comparison of the detected fluctuation modes in the two ferriphases to calculated selection rules for their coupling to light are consistent with the distorted clock structures recently reported by an optical ellipsometry study, but indicate that the distortion has a polar component in both ferriphases. We also find a surprisingly large amplitude and dispersion associated with scattering from fluctuations in the tilt angle magnitude. In terms of the discrete interlayer interaction models currently being used to account for the ferriphases, this finding suggests that the interlayer interaction coefficients are of comparable magnitude to the intralayer coefficients that stabilize the tilt angle.

DOI: 10.1103/PhysRevE.64.010704

PACS number(s): 61.30.Eb, 61.30.Cz, 78.35.+c

The discovery of two ferroelectric phases in chiral smectic liquid crystals [1] demonstrates that rather complex interlayer ordering of molecular dipoles can occur in a system lacking true long-range positional order. The precise dipolar arrangement in the ferroelectric phases has been the subject of intensive experimental study. These phases, designated  $\text{Sm}C_{FI1}$  and  $\text{Sm}C_{FI2}$ , lie between the antiferroelectric ( $\text{Sm}C_A^*$ ) and ferroelectric ( $\text{Sm}C^*$ ) phases. Although an elegant resonant x-ray scattering experiment [2] performed on freely-suspended (FS) thin films proved that the  $\text{Sm}C_{FI1}$  and  $\text{Sm}C_{FI2}$  phases are characterized by superlattices of three and four smectic layers, respectively, determining the full details of the interlayer director ordering from x-ray line-shapes alone has not yet been possible. In particular, the type and degree of distortion of the interlayer orientational structure from the simplest, symmetric “clock” model (in which the tilted director precesses with a constant angular increment of  $120^\circ$  or  $90^\circ$  between smectic layers) remain uncertain issues in the x-ray studies. However, a recent optical ellipsometry study [3] on FS films reveals a highly distorted clock structure in both ferriphases, deduced mainly from the detection of optical biaxiality.

In this Rapid Communication, we present a study of the dynamics of the ferriphases in a liquid crystal where the known size of the optical unit cell allows a detailed analysis of the number and type of director fluctuation modes, and an explicit calculation of the selection rules that determine their relative contributions to the measured light scattering cross section. We demonstrate that dynamic light scattering provides a simple method for distinguishing between symmetric, nonpolar asymmetric, and polar asymmetric orientational structure in the  $\text{Sm}C_{FI1}$  and  $C_{FI2}$  phases. Unlike the FS film studies, we study a bulk sample consisting of many thousand smectic layers confined in an ordinary electro-optical cell, which is the situation most likely to be of interest in any technological application of these materials. Our specific results, obtained on a sample aligned in the “bookshelf” layer geometry, are consistent with the conclusions of the ellip-

sometry study in FS films, except for a polar component to the orientational structure of the  $\text{Sm}C_{FI2}$  phase. We also observe an unusually significant degree of scattering from fluctuations in the *magnitude* of the tilt order parameter, and discuss the implication of this finding for Landau-deGennes theories of the ferriphases.

The structure of the ferriphases can be described in terms of the orientational variation between layers of the in-plane component of the molecular director, which is inclined on average by an angle  $\theta$  with respect to the smectic layer normal. We denote the orientation of this component for layer  $j$  by  $\phi_j$  (measured from a fixed reference axis). When the increments in  $\phi_j$  between layers are the same and equal to  $360^\circ/N$  for some integer  $N$ , one has a symmetric clock structure with an optical unit cell of  $N$  molecules. When the increments are not the same for all  $j$ , one has an asymmetric or distorted clock structure. Distorted structures for  $N=2,3$  are shown in Fig. 1 (top). The distortion is described by a single angle  $\Delta_p$ , which in both cases gives rise to a polar unit cell (i.e., the in-plane director summed over a unit cell is non-zero). The limiting cases corresponding to planar or “Ising”-like structures are given by  $\Delta_p=0^\circ$  or  $90^\circ$  (for  $N=2$ ) and  $\Delta_p=60^\circ$  or  $-120^\circ$  (for  $N=3$ ). For  $N=4$ , as shown in Fig. 1 (bottom), polar and nonpolar distortions may be comprehensively described by a set of distortion angles  $(\Delta_{P1}, \Delta_{P2}, \Delta_{NP})$ . The “Ising” model limits are given by the sets  $(0^\circ, 90^\circ, 0^\circ)$  and  $(90^\circ, 90^\circ, 90^\circ)$  (polar unit cell), and  $(0^\circ, 0^\circ, 90^\circ)$  (nonpolar unit cell). In all cases a bulk chiral structure may be superposed on the microscopic orientational structure. This produces a small additional angular increment,  $\Delta_H$ , between neighboring layers.

The structure function  $S(\vec{q})$  for depolarized light scattering may be calculated in terms of the director fluctuations  $\delta\theta_j, \delta\phi_j$  with wave vector  $\vec{q}$  after first making simplifying assumptions appropriate to our experimental conditions. We chose the polarizer perpendicular to the scattering ( $y-z$ ) plane and the analyzer parallel to it. Since the optical scattering vector ( $\approx 10 \mu\text{m}^{-1}$ ) is much less than the reciprocal

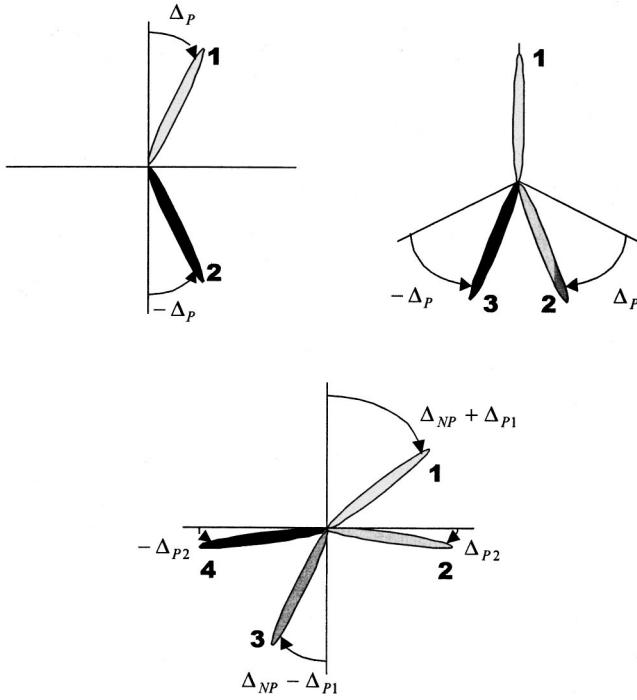


FIG. 1. Polar ( $\Delta_P$ ) and nonpolar ( $\Delta_{NP}$ ) distortions of a symmetric “clock” in-layer director structure for the  $\text{SmC}_A$ ,  $C_{FI1}$ , and  $C_{FI2}$  phases, with optical unit cells containing 2, 3, and 4 molecules, respectively. (The figure does not include the small increments due to the macroscopic chiral helix.)

lattice vector ( $2\pi/(Nd) \sim 600 \mu\text{m}^{-1}$ ,  $d =$  smectic layer spacing),  $S$  effectively contains an average over the  $N$ -fold unit cell. Combining this with a wave vector for the chiral helix,  $\vec{q}_0 = (\Delta_H/d)\hat{z}$ , also in the optical range, we find  $S$  to be the sum of two terms,

$$S_{xz}(\vec{q} \pm \vec{q}_0) = \left\langle \left| \frac{\epsilon_a}{2N} \sum_{j=1}^N [\cos 2\theta_0 \delta\theta_j(\vec{q} \pm \vec{q}_0) \pm i \sin \theta_0 \cos \theta_0 \delta\phi_j(\vec{q} \pm \vec{q}_0)] e^{\pm i\phi_{0j}} \cos \theta_s \right|^2 \right\rangle, \quad (1)$$

$$S_{xy}(\vec{q} \pm 2\vec{q}_0) = \left\langle \left| \frac{\epsilon_a}{2N} \sum_{j=1}^N [\mp i \sin \theta_0 \cos \theta_0 \delta\theta_j(\vec{q} \pm 2\vec{q}_0) + \sin^2 \theta_0 \delta\phi_j(\vec{q} \pm 2\vec{q}_0)] e^{\pm i2\phi_{0j}} \sin \theta_s \right|^2 \right\rangle,$$

where  $\epsilon_a$  is the dielectric anisotropy (neglecting biaxiality),  $\theta_0$ ,  $\phi_{0j}$  are the equilibrium tilt and phase angles, and  $\theta_s$  is the scattering angle in the sample. Equation (1) indicates that the scattering in  $\vec{q}$  space is centered on the helical wave vectors  $\pm\vec{q}_0$  and  $\pm 2\vec{q}_0$  [4].

We can use the above results to calculate scattering selection rules for the normal modes of the structures shown in Fig. 1. We shall illustrate in detail results for the lower fre-

quency modes—those involving fluctuations  $\delta\phi_j$  in the phase of the tilt order parameter. For the twofold structure ( $N=2$ ), we have a single acousticlike mode corresponding to in-phase orientational fluctuations,  $1/\sqrt{2}(\delta\phi_1, \delta\phi_2)$ , and a single opticlike mode for out-of-phase fluctuations,  $1/\sqrt{2}(\delta\phi_1, -\delta\phi_2)$  [5]. The equilibrium orientations are  $\phi_{01} = \Delta_P$ ,  $\phi_{02} = 180^\circ - \Delta_P$ . For  $N=3$ , we have one acousticlike mode and two opticlike modes (see the first column of Table I), and  $\phi_{01} = 0$ ,  $\phi_{02} = 120^\circ + \Delta_P$ ,  $\phi_{03} = 240^\circ - \Delta_P$ . Here, and throughout the table, explicit values of the index  $j$  correspond to the labels 1-4 in Fig. 1. Finally, for  $N=4$ , we have an acousticlike mode and three opticlike modes, and  $\phi_{01} = \Delta_{NP} + \Delta_{P1}$ ,  $\phi_{02} = 90^\circ + \Delta_{P2}$ ,  $\phi_{03} = 180^\circ + \Delta_{NP} - \Delta_{P1}$ ,  $\phi_{04} = 270^\circ - \Delta_{P2}$ . The scattering selection rules for these cases (assuming small equilibrium tilt  $\sin \theta_0 \approx \theta_0, \cos \theta_0 \approx 1$ ) are also presented in the table. The specific entries in the table corresponds to the “form” factors, which multiply the mean-square amplitudes of the individual normal modes contributing to the structure factor components in Eq. (1). (The phase angle increment  $\Delta_H$  due to the chiral helix has been neglected under the assumption that it is small compared to the increment in  $\phi_{0j}$  between layers.) We observe that the relative values of the coupling factors in the table depend on the details of the ferriphase structure. In particular, the acoustic mode contributes to the  $S_{xz}$  scattering *only when the structure is asymmetric and has a polar component. The presence of acoustic mode scattering in  $S_{xz}$  then rules out a symmetric clock structure* [6].

Let us now turn to the details of our light-scattering experiment. Our measurements were conducted on a  $10\text{-}\mu\text{m}$  thick sample of R-10OTBBB1M7. The bulk phase sequence is [7]  $\text{SmC}_A^*(112.0)$   $\text{SmC}_{FI1}$  (114.0)  $\text{SmC}_{FI2}$  (119.2)  $\text{SmC}^*$  (120.2)  $\text{SmC}_\alpha$  (123.6°C)  $\text{SmA}$ . The sample was sandwiched between glass slides with the smectic layer normal parallel to the substrates (“bookshelf” geometry). A single orientational domain was obtained with the help of a square-wave electric field applied briefly on cooling first into the  $\text{SmA}$  and then later in the  $\text{SmC}_A$  phases. The time-correlation function of the 488-nm scattered light was recorded in a depolarized, forward-scattering geometry with the smectic layer normal  $\hat{z}$  lying in the scattering plane. The scattering vector  $\vec{q} = q_z \hat{z}$  was varied between 1.8 and  $10.2 \mu\text{m}^{-1}$ . In this range we probe mainly the  $\vec{q}_0$  branch of the scattering (i.e.,  $S_{xz}$ ); in fact we estimate from Eqs. (1) and (2) that the ratio of  $2\vec{q}_0$  to  $\vec{q}_0$  scattering did not exceed 3% for any fluctuation mode. Temperatures for the transitions between antiferro-, ferri-, and ferroelectric phases were previously determined by high-resolution heat capacity and electro-optical studies on bulk R-10OTBBB1M7 [7]. We also performed our own calorimetry to confirm consistency with the published temperatures.

Our data for the dispersion of the director fluctuation modes detected in the  $\text{SmC}_A$ ,  $\text{SmC}_{FI1}$ , and  $\text{SmC}_{FI2}$  phases are presented in Fig. 2. In the  $\text{SmC}_A$  phase ( $T = 110.0^\circ\text{C}$ ), a high frequency ( $10^6 \text{sec}^{-1}$ ) opticlike mode and a moderate frequency ( $10^4\text{--}10^5 \text{sec}^{-1}$ ) optic mode are detected. Both modes are centered on a wave vector  $q_z$  well away from zero and consistent with the observed position of a weak diffrac-

TABLE I. Selection rules for depolarized light scattering from phase angle fluctuation modes in the  $\text{SmC}_A$ ,  $\text{SmC}_{F11}$ , and  $\text{SmC}_{F12}$  phases.

Mode	$S_{xz}(\vec{q} \pm \vec{q}_0)$	$S_{xy}(\vec{q} \pm 2\vec{q}_0)$
$\frac{1}{\sqrt{2}}(\delta\phi_1, \delta\phi_2)$	$\frac{1}{2}\theta_0^2\sin^2\Delta_P$	$\frac{1}{2}\theta_0^4\cos^22\Delta_P$
$\frac{1}{\sqrt{2}}(\delta\phi_1, -\delta\phi_2)$	$\frac{1}{2}\theta_0^2\cos^2\Delta_P$	$\frac{1}{2}\theta_0^4\sin^22\Delta_P$
$\frac{1}{\sqrt{3}}(\delta\phi_1, \delta\phi_2, \delta\phi_3)$	$\frac{1}{3}\theta_0^2(1 - \cos\Delta_P - \sqrt{3}\sin\Delta_P)^2$	$\frac{1}{3}\theta_0^4(1 - \cos2\Delta_P + \sqrt{3}\sin2\Delta_P)^2$
$\frac{1}{\sqrt{6}}(2\delta\phi_1, -\delta\phi_2, -\delta\phi_3)$	$\frac{1}{6}\theta_0^2(2 + \cos\Delta_P + \sqrt{3}\sin\Delta_P)^2$	$\frac{1}{6}\theta_0^4(2 + \cos2\Delta_P - \sqrt{3}\sin2\Delta_P)^2$
$\frac{1}{\sqrt{2}}(0, \delta\phi_2, -\delta\phi_3)$	$\frac{1}{2}\theta_0^2(\sqrt{3}\cos\Delta_P - \sin\Delta_P)^2$	$\frac{1}{2}\theta_0^4(\sqrt{3}\cos2\Delta_P + \sin2\Delta_P)^2$
$\frac{1}{2}(\delta\phi_1, \delta\phi_2, \delta\phi_3, \delta\phi_4)$	$\frac{1}{4}\theta_0^2(\sin^2\Delta_{P1} + \sin^2\Delta_{P2} + 2\sin\Delta_{P1}\sin\Delta_{P2}\sin\Delta_{NP})$	$\frac{1}{4}\theta_0^4(\cos^22\Delta_{P1} + \cos^22\Delta_{P2} - 2\cos2\Delta_{P1}\cos2\Delta_{P2}\cos2\Delta_{NP})$
$\frac{1}{2}(\delta\phi_1, -\delta\phi_2, -\delta\phi_3, \delta\phi_4)$	$\frac{1}{4}\theta_0^2(\cos^2\Delta_{P1} + \cos^2\Delta_{P2} - 2\cos\Delta_{P1}\cos\Delta_{P2}\sin\Delta_{NP})$	$\frac{1}{4}\theta_0^4(\sin^22\Delta_{P1} + \sin^22\Delta_{P2} + 2\sin2\Delta_{P1}\sin2\Delta_{P2}\cos2\Delta_{NP})$
$\frac{1}{2}(\delta\phi_1, \delta\phi_2, -\delta\phi_3, -\delta\phi_4)$	$\frac{1}{4}\theta_0^2(\cos^2\Delta_{P1} + \sin^2\Delta_{P2} + 2\cos\Delta_{P1}\cos\Delta_{P2}\sin\Delta_{NP})$	$\frac{1}{4}\theta_0^4(\sin^22\Delta_{P1} + \sin^22\Delta_{P2} - 2\sin2\Delta_{P1}\sin2\Delta_{P2}\cos2\Delta_{NP})$
$\frac{1}{2}(\delta\phi_1, -\delta\phi_2, \delta\phi_3, -\delta\phi_4)$	$\frac{1}{4}\theta_0^2(\sin^2\Delta_{P1} + \sin^2\Delta_{P2} - 2\sin\Delta_{P1}\sin\Delta_{P2}\sin\Delta_{NP})$	$\frac{1}{4}\theta_0^4(\cos^22\Delta_{P1} + \cos^22\Delta_{P2} + 2\cos2\Delta_{P1}\cos2\Delta_{P2}\cos2\Delta_{NP})$

tion spot due to the chiral helix. The solid lines are fits of the inverse relaxation time to a parabolic dispersion,  $\tau^{-1} \sim (q_z - q_0)^2$ , and yield  $q_0 = 9 \mu\text{m}^{-1}$  or an optical pitch of approximately  $0.7 \mu\text{m}$ . From the table, the absence of a low-frequency (gapless) acoustic mode implies  $\Delta_P \approx 0^\circ$ —i.e., a symmetric twofold structure with  $180^\circ$  rotational symmetry. Then the only phase fluctuation mode expected is an optic mode  $[1/\sqrt{2}(\delta\phi_1, -\delta\phi_2)]$ , which we assign to the lower frequency of the two observed modes. The higher frequency mode must then arise from fluctuations in the tilt angle *magnitude*; in fact, the frequency and dispersion of this mode are quite consistent with that of the single mode observed at higher temperature near the  $\text{SmA}$  phase, where the dominant scattering should be due to tilt fluctuations. Although two tilt modes generally contribute in Eq. (1), for  $\Delta_P = 0^\circ$  only one is observable. Our detection of a tilt modes at a frequency 10 times greater (and therefore an intrinsic amplitude  $\sim 10$  times less) than the phase mode is explained by Eq. (1), where we see that the cross section for tilt fluctuations is enhanced by a factor  $1/\theta_0^2 \sim 10$  relative to the phase fluctuations.

Turning now to the  $\text{SmC}_{F11}$  ferriphase (at  $T = 113.3^\circ\text{C}$ ), we continue to observe both the high-frequency tilt and optic phase modes, with relaxation rates  $\tau^{-1}$  basically unchanged from the  $C_A$  phase. From parabolic fits to these modes, we get  $q_0 = 8 \mu\text{m}^{-1}$ . However, an additional, much lower frequency phase mode is also detected. This mode has a gap of order  $10^3 \text{sec}^{-1}$ , and is consistent with the acoustic phase mode, where the observed residual gap is due to the fact that we could not study  $q_z = q_0$  precisely because of the large amount of static scattering coming from the diffraction spot at  $q_0$ . We confirmed this identification of the acoustic mode

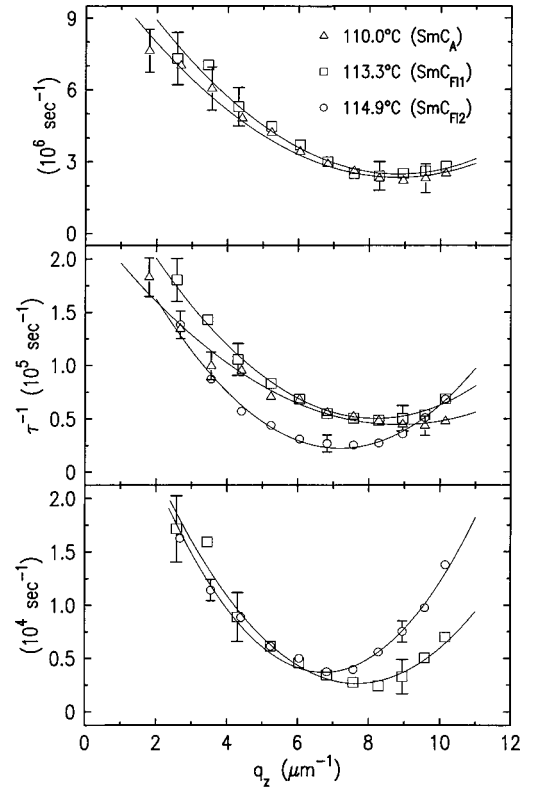


FIG. 2. Dispersion of the relaxation rates ( $\tau^{-1}$ ) for the tilt (top), opticlike phase (middle), and acousticlike phase (bottom) modes observed in the ferriphases of R-10OTBBB1M7. The scattering vector  $q_z$  is along the smectic layer normal. Solid lines represent parabolic fits,  $\tau^{-1} \sim (q_x - q_0)^2$ , centered on the wave vector  $q_0$  of the chiral helix.

by tracking it into the narrow ferroelectric phase, where the acoustic scattering completely dominates the spectrum [4]. From the selection rules in the table, the presence of acoustic mode scattering centered on  $q_0$  immediately implies that the  $\text{SmC}_{FI1}$  phase must have polar asymmetry. Moreover, the detection of a single optic phase mode suggests that the asymmetry is quite large. Specifically, from the Table I, we see that one of the two optic phase modes has a vanishing cross section on the  $\vec{q}_0$  branch when  $\Delta_P \rightarrow 60^\circ$ . In fact, we can use the results of the table, the measured acoustic and optic phase mode frequencies, and the measured relative amplitudes to extract a value of  $\Delta_P$ . Applying this to the results of our correlation fits for all  $\vec{q}$  studied, we find  $\Delta_P = 45_{-10}^{+15}$ . The reason for the large error bar is twofold. First, the fact that the tilt mode is at the edge of our correlator's range makes the amplitudes of all the modes somewhat more uncertain than normal. Second, the ratio of cross sections in the table varies by only 20% for  $45^\circ < \Delta_P \leq 60^\circ$ . But the main point, that the  $\text{SmC}_{FI1}$  phase is highly distorted from the symmetric ‘‘clock’’ model, is now confirmed by a dynamical measurement.

In the  $\text{SmC}_{FI2}$  phase ( $T = 114.9^\circ\text{C}$ ), only the lower frequency modes (centered on  $q_0 \approx 7\mu\text{m}^{-1}$ ) are observed for all values of  $q_z$ . The tilt fluctuations were only detected when  $q_z \ll q_0$ . The two low frequency modes are similar in behavior to the acoustic and optic phasons of the  $C_{FI1}$  phase, and, from the table, the detection of acoustic scattering again implies polar asymmetry for the  $C_{FI2}$  phase (i.e., nonzero  $\Delta_{P1}$  or  $\Delta_{P2}$ ). This rules out the symmetric clock and nonpolar Ising models. We can also rule out the polar Ising model, since results from the table for this model combined with the measured ratio of relaxation rates predict an acoustic to optic mode amplitude ratio  $\sim 10$  times higher than measured. Thus, our light-scattering measurements support a distorted clock model with intermediate values of the distortion

angles. Without more comprehensive data, we are not currently able to make separate estimates of the polar and nonpolar distortion angles; however, we note from the table that for large  $\Delta_{NP}$  (i.e.,  $\Delta_{NP} \rightarrow 90^\circ$ ), the optic phase mode scattering should reduce to a single observable mode, as is indeed the case in our experimental results. If we use the value  $\Delta_{NP} \approx 65^\circ$  [8] reported from ellipsometry on a FS film of 10OTBBB1M7, and assume the simplest case where  $\Delta_{P1} = \Delta_{P2} = \Delta_P$ , our measurements of the phase mode amplitudes and relaxation rates imply  $\Delta_P \approx 15^\circ$ . Because of the different dependences of the mode amplitudes on distortion angles indicated in the table, improved estimates of these angles should be possible by probing *both* the  $\vec{q}_0$  and  $2\vec{q}_0$  branches of the scattering on the same sample.

We conclude by briefly considering the relatively large dispersion [9] associated with the tilt fluctuation mode, which we observed in the ferriphases (and also in the  $\text{SmC}_\alpha$  and  $A$  phases). The large dispersion has implications for the relative magnitude of the coefficients appearing in Landau-deGennes-type expansions of the free energy of the ferriphases. The most promising of these (for predicting known structural properties and phase sequences) are based on discrete, near-neighbor interactions between layers, similar to ANNNI models [10]. The free energy contains ‘‘mean-field’’ or intralayer terms of the form  $a_0\theta_j^2 + b_0\theta_j^4$  (which stabilize the tilted structure) plus interlayer interaction terms like  $a_j\theta_j\theta_{j+1}\cos(\phi_j - \phi_{j+1})$  (which stabilize the various ferriphase structures). A large tilt mode dispersion then basically means that the interlayer coefficients  $a_j$  (which set the curvature of the dispersion) and the intralayer coefficients  $a_0$  (which set the gap) have comparable magnitude.

This research was supported by the NSF under Grant Nos. DMR-8920147 and DMR-9904321. We are grateful to R. Pindak and C. C. Huang for helpful conversations.

- 
- [1] A. Fukuda, Y. Takanishi, T. Isozaki, K. Ishikawa, and H. Takazoe, *J. Mater. Chem.* **4**, 997 (1994).
- [2] P. Mach, R. Pindak, A. Levelut, P. Barois, T. Nguyen, H. Baltes, M. Hird, K. Toyne, A. Seed, J. Goodby, C. Huang, and L. Furenlid, *Phys. Rev. E* **60**, 6793 (1999); P. Mach, R. Pindak, A.-M. Levelut, P. Barois, H.T. Nguyen, C.C. Huang, and L. Furenlid, *Phys. Rev. Lett.* **81**, 1015 (1998).
- [3] P.M. Johnson, D.A. Olson, S. Pankratz, T. Nguyen, J. Goodby, M. Hird, and C.C. Huang, *Phys. Rev. Lett.* **84**, 4870 (2000).
- [4] I. Drevensek, I. Musevic, and M. Copic, *Phys. Rev. A* **41**, 923 (1990); I. Musevic, R. Blinc, B. Žekš, C. Filipic, M. Copic, A. Seppen, P. Wyder, and A. Levanyuk, *Phys. Rev. Lett.* **60**, 1530 (1988).
- [5] I. Mušević, A. Rastegar, M. Čepič, B. Žekš, M. Čopič, D. Moro, and G. Heppke, *Phys. Rev. Lett.* **77**, 1769 (1996).
- [6] In principle, a symmetric structure with  $\Delta_P = \Delta_{NP} = 0$  but  $\Delta_H \neq 0$  could still give acoustic scattering, but its amplitude relative to the optic modes would scale with  $\sin^2\Delta_H \approx \Delta_H^2 \approx 0.006$ , so that, practically, the acoustic mode would be too weak to detect.
- [7] H.T. Nguyen, J.C. Rouillon, P. Cluzeau, G. Sigaud, C. Destrade, and N. Isaert, *Liq. Cryst.* **17**, 571 (1994).
- [8] C.C. Huang (private communication).
- [9] At similar frequencies near typical  $A - C$  transitions, this mode has much weaker dispersion.
- [10] M. Skarabot, M. Čepič, B. Žekš, R. Blinc, G. Heppke, A. Kityk, and I. Mušević, *Phys. Rev. E* **58**, 575 (1998); M. Čepič and B. Žekš, *Liq. Cryst.* **20**, 29 (1996); H. Orihara and Y. Ishibashi, *Jpn. J. Appl. Phys.* **29**, L115 (1990).